Optical Engineering

OpticalEngineering.SPIEDigitalLibrary.org

Trapping efficiency of fluorescent optical fibers

Jonathan D. Weiss

SPIE.

Trapping efficiency of fluorescent optical fibers

Jonathan D. Weiss*
JSA Photonics, LLC, 439 Tayne Lane, P.O. Box 2930, Corrales, New Mexico 87048, United States

Abstract. Fluorescent optical fibers are used in nuclear detection and other forms of fiber-optic sensors. The trapping efficiency of a fluorescent optical fiber is defined by the optical energy trapped (or guided) by the fiber divided by the total energy emitted within it by the fluorescers that dope the fiber core. This characteristic is clearly important in determining the size of signals from these devices. A calculation of the trapping efficiency has been performed under the assumption that the fluorescence radiation is emitted isotropically by the individual fluorescers that are uniformly distributed throughout the core and are equally likely to be excited by particles or shorter-wavelength light. At the price of increased complexity, nothing in the analysis precludes the lifting of these restrictions. What is included in this analysis is the contribution of skew rays, which, to the author's knowledge, is not presented elsewhere. A very simple expression for the trapping efficiency as a function of the cladding-to-core index ratio is derived. Also important in determining signal size is the transmission loss of the fluorescence radiation to either end of the fiber from the point of its generation. However, as it is a separate matter, it is not discussed here. [DOI: 10.1117/1.OE.54.2.027101]

Keywords: optical fibers; fluorescence; optical detectors; solid scintillation detectors.

Paper 141787 received Nov. 21, 2014; accepted for publication Jan. 27, 2015; published online Feb. 17, 2015.

1 Introduction

Plastic fluorescent optical fibers have been widely discussed in detail as nuclear particle detectors as a result of the scintillation radiation they produce in their interior when bombarded with such particles. Some of the light travels to either end of the fiber, where it generates an electrical signal in a photodetector. Four examples of such discussions are in Refs. 1–4, along with a textbook on radiation detection.[5] Fluorescent fibers are also used in at least one optical sensor that is unrelated to particle detection.[6] In this case, the fluorescence at a given wavelength is generated by a pump light of a shorter wavelength operating continuously. Saint Gobain[7] and Nanoptics[8] are two companies that manufacture fluorescent fibers.

The fraction of the fluorescence power generated within the fiber that is trapped or guided by it is the subject of this paper. Its practical importance lies in its contribution to the size of the signal in the above applications, along with the contribution from the attenuation of the guided power between the points of generation and detection. Scattering or absorption of the fluorescence radiation by the fluorescers themselves adds to the attenuation caused by the bulk material of the fiber. Although the wavelength- and fluorescer-dependent loss of the signal during propagation will not be considered here, as it is a completely separate matter, measurements of transmission loss are presented in Refs. 3, 4, and 7.

2 Initial Considerations of the Trapped Power

Before presenting the calculation of the trapped power, we state our assumptions that form the basis for that calculation. The first is that the fluorescers are uniformly distributed throughout the fiber core and that the distribution can be characterized by a volume density, ρ, of fluorescers. The second is that the fluorescers emit radiation isotropically into 4π steradians. The third is that they are equally likely to emit, which means that the stimulus is uniform throughout the fiber cross-section, at least on a time-average basis. The stimulus, I, can be thought of as an optical power per unit area or the number of particles crossing a unit area per unit time. If the probability of emission per unit stimulus and per unit solid angle is p, then the probability of emission per unit solid angle is pI. The last is that the fibers are highly multimode. In other words, they have a large enough diameter and numerical aperture that a ray-optics treatment is completely adequate.

The first and fourth assumptions are eminently reasonable. The second assumption could be a bit of an oversimplification because the fluorescers may emit dipole radiation, which is not isotropic. On the other hand, if they are randomly oriented in a small macroscopic volume, their angular average could be close to isotropic. To determine the details of emission, one would have to examine how fluorescent dye molecules are incorporated into a polymer matrix, such as with respect to their alignment, and how those molecules respond to various stimuli, I. The third assumption is one of linearity, which is valid for small enough stimuli. Are the stimuli encountered in practice likely to be small enough for linearity to hold? Incorporating the answers to these questions into a calculation of the trapping efficiency is outside the scope of this paper and is almost certain to require a numerical approach. However, doing so may provide an illuminating comparison to the results obtained in this self-contained, analytic treatment.

Based on these assumptions, we can readily see that the total fluorescent power per unit thickness of fiber, P_T, is

*Address all correspondence to: Jonathan D. Weiss, E-mail: jondweiss@aol.com

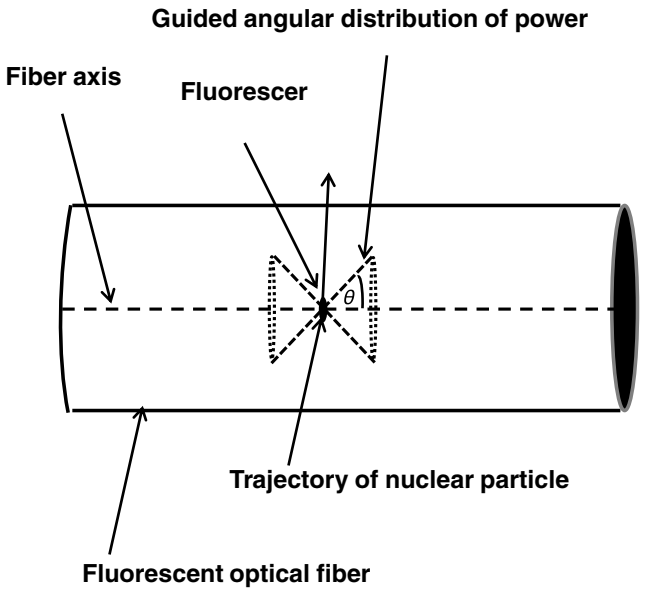

Fig. 1 Emission of guided radiation from an on-axis fluorescer within a fluorescent optical fiber.

$$P_T = (\pi a^2)(4\pi)(\rho)(pI). \tag{1}$$

In this equation, a is the fiber radius. When considering the trapping efficiency, the explanation provided by, for example, Saint Gobain, is as shown in Fig. 1.

A particle excites a fluorescer located along the fiber axis that consequently emits over an angle θ, such that the radiation is guided. The condition for guidance or total internal reflection (TIR) is that $\cos\theta > n_{cl}/n_{co}$, where the two refractive indices refer to the core and cladding (1.6 and 1.49, for the Saint Gobain fiber). Then the fraction of the total power emitted by these axial fluorescers (P_f) that is guided can easily be shown to be

$$P_f = 1 - \cos\theta = 1 - n_{cl}/n_{co}, \tag{2}$$

where θ is the maximum angle of emission that leads to guidance. For these core and cladding indices, Eq. (2) yields 6.88% and a maximum emission angle of ≈21.4 deg. The percentage is the total for both forward and backward propagation of the fluorescence radiation. The result is, however, a simplification because it leaves out the off-axis sources of fluorescence. These off-axis sources produce skew rays, which corkscrew their way along the fiber while never crossing the axis, as opposed to the meridional rays that always cross the axis. The on-axis sources only produce meridional rays. Both of these are depicted in Fig. 2.

It is mentioned in Ref. 7 that ~7% of the emission originating near the core-cladding interface will be guided, and passing consideration is given to them in Ref. 5. To the author's knowledge, however, no quantitative analysis of the trapping efficiency has been published that includes skew rays. We now turn our attention to them.

3 Skew Rays

We should first note that because of the continuous distribution of fluorescers within the fiber core and their continuous emission over angles, all but an infinitesimal fraction of the

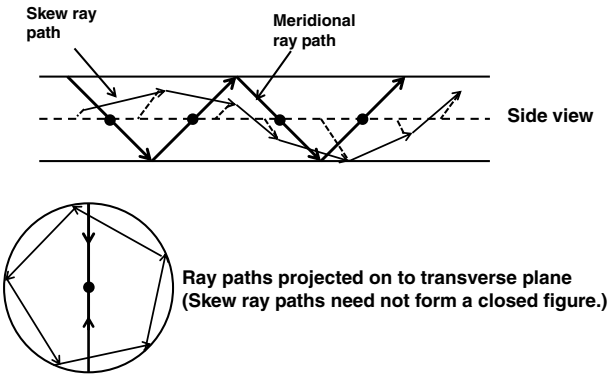

Fig. 2 Skew and meridional ray paths within an optical fiber.

fluorescent radiation is in the form of skew rays. What is critical about skew rays in the context of trapping efficiency is the fact that their angle of incidence at the core-cladding interface depends on their azimuth, as well as their elevation ($\pi/2 - \theta$). Their azimuthal angle is φ in Fig. 3, where, in a perspective view, a skew ray is shown emerging from a fluorescer at a distance r from the center of the fiber, along an arbitrary radius.

The angle α is that between the horizontal projection of the skew ray and the radius of the fiber. The angle of incidence is the slant angle β, which is larger than it would be if φ were 0 or π radians. If it were either, then the skew ray would be a meridional ray. Thus, skew rays may be incident at an angle greater than the critical angle over part, all, or none of the range of φ, depending on r and θ. This added TIR is the basis of the comment in Ref. 7 as mentioned above. Taking projections of the skew ray onto the horizontal plane and the radius, we obtain:

$$\cos\beta = \sin\theta\cos\alpha. \tag{3}$$

Based on the law of sines,

$$\sin\alpha = \frac{r\sin\varphi}{a}. \tag{4}$$

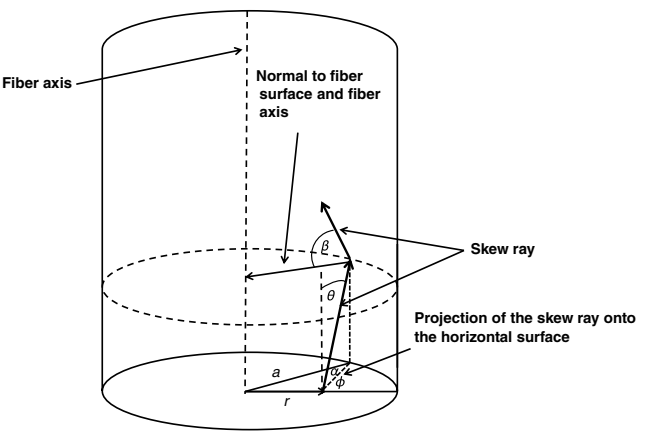

Fig. 3 Geometry of a skew ray.

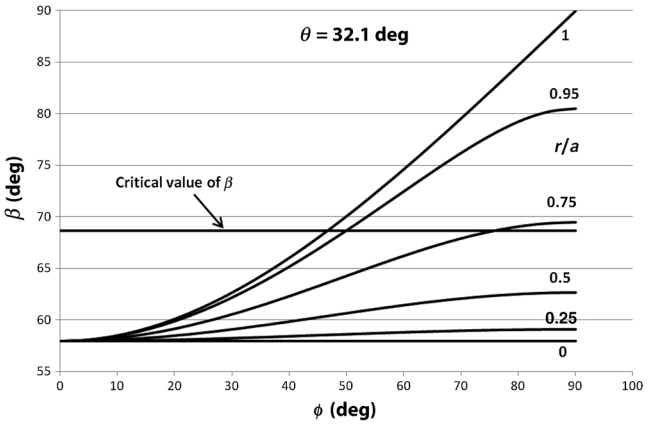

Fig. 4 Angle of incidence, β, versus azimuthal angle, φ, for various values of (r/a) and for $\theta = 32.1$ deg.

Thus,

$$\cos\beta = \sin\theta\sqrt{1-(r\sin\varphi/a)^2}. \tag{5}$$

It is clear from this equation that the angle of incidence is smallest when (r/a) or $\sin\varphi$, or both are zero. It then increases as the product of these two factors increases, reaching 90 deg when the product is unity. This implies that if θ is small enough ($\theta \leq 21.4$ deg for Saint Gobain fibers) to initially allow for TIR, then TIR will exist throughout the entire range of φ and (r/a). The behavior of the angle of incidence is shown in Figs. 4 and Fig. 5, which are graphs of β versus φ.

In Fig. 4, the value of θ for all curves is 32.1 deg, or 1.5 times the largest angle that allows for TIR when $(r/a)\sin\varphi$ is zero. Thus, $\beta <$ the critical angle for some range of φ. For the smaller values of (r/a), this is true over the entire range of φ. However, for $(r/a) = 0.75$ and 0.95, respectively, TIR does occur for $\varphi > \sim 76$ and ~ 45 deg.

In Fig. 5, the value of $(r/a) = 0.5$ for all curves, but θ is allowed to vary upward in the immediate vicinity of 21.4 deg. At 21.4 deg, TIR occurs for all φ. As θ increases, the crossover to TIR occurs at progressively larger values of φ. At $\theta = 22.6$ deg, for example, TIR only occurs for $\varphi > \sim 40$ deg. At $\theta = 24.9$ deg, no TIR occurs for any value of φ.

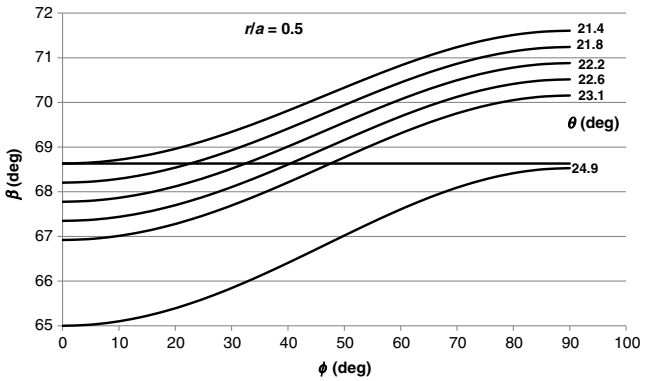

Fig. 5 Angle of incidence, β, versus azimuthal angle, φ, for various values of θ and for $(r/a) = 0.5$.

Before presenting the calculation of the trapping efficiency based on the above considerations, we should note only for completeness that very technically, skew rays that would not be guided if they were meridional rays are not guided in a round fiber, even if they satisfy the condition for TIR at the point of incidence. The reason for this is because for skew rays, the boundary is curved in their plane of incidence and Fresnel's laws of reflection are valid only for a planar boundary. The result is that although these rays are predicted to experience TIR, they lose energy by tunneling out of the core. For a radius of curvature of the boundary that is much larger than the wavelength of light, which is certainly the case here, the loss is extremely gradual with the propagation distance and is only of consequence over many kilometers of fiber length, which is certainly not the case here. It should also be noted that when these rays are predicted to refract out of the core, they do so even in the case of a curved boundary. The curved boundary is of no practical consequence here and is being ignored. The whole notion of tunneling or weakly leaky rays was developed by Snyder and coworkers in the 1970s and is discussed in Ref. 9 and the references contained therein.

4 Calculation of the Trapping Efficiency

As stated earlier, the trapping efficiency is the fraction of the total power emitted in 4π steradians by all fluorescers per unit length that is guided by the fiber. We break up the power that is guided into those rays that are emitted into an angle $0 \leq \theta \leq \theta_o$ (referred to here as narrow-angle rays) and those for which $(\pi/2) \geq \theta \geq \theta_o$ (or wide-angle rays). For Saint Gobain fibers, $\theta_o \approx 21.4$ deg. The contribution of the narrow-angle rays to the total guided optical power, P_N, is

$$P_N = (\pi a^2)(2)(2\pi)(\rho)(pI)\left(1-\frac{n_{cl}}{n_{co}}\right). \tag{6}$$

The numerical prefactors involve the area of the fiber, the propagation forward and backward, and the integral over φ. To obtain the fraction of the total power, we divide P_N by P_T in Eq. (1). The additional contribution is from wide-angle rays and for which $\beta \geq \beta_{crit}$, the critical angle over some range of φ and (r/a). We now consider that contribution, denoted by P_W. We note that

$$\cos\beta_{crit} = \sin\theta_o = \mathrm{NA}/n_{co}, \tag{7}$$

where the numerical aperture of the fiber, NA, is $\{n_{co}^2 - n_{cl}^2\}^{(1/2)}$. Since $\beta \geq \beta_{crit}$, $\cos\beta \leq \cos\beta_{crit}$. This condition and the one on wide-angle rays, $\sin\theta_o > \mathrm{NA}/n_{co}$, form the basis for calculating the contribution to the guided power from these rays. The calculation will involve φ up to $\pi/2$, even though it extends to 2π. By symmetry, the result can be multiplied by 4. It is then multiplied by 2 because both forward and backward propagation are being included. Finally, it is multiplied by 2π to include the angular contribution to the circular area of the fiber. The prefactor is then $16\pi\rho pI$. This prefactor is then multiplied by a triple integral involving the solid angle over which ray emission takes place and the range of the radial position of the fluorescer. The resulting expression for P_W is

$$P_W = 16\pi\rho pI \int_{\theta_L}^{\theta_U} \sin\theta d\theta \int_{\varphi_L}^{\varphi_U} d\varphi \int_{\left(\frac{r}{a}\right)_L}^{\left(\frac{r}{a}\right)_U} (a^2)\left(\frac{r}{a}\right) d\left(\frac{r}{a}\right). \tag{8}$$

We should note that the order of the integration over φ and (r/a) can be reversed, such that the integral over φ is first. The result is unchanged. The values of θ_U and φ_U are $\pi/2$ for reasons discussed above. The value of $(r/a)_U$ is obviously 1. The value of θ_L is $\sin^{-1}(NA/n_{co})$ because we are considering only wide-angle rays. The lower limit of (r/a), $(r/a)_L$, is determined from Eq. (7), and $\beta > \beta_{crit}$. The result is that

$$\left(\frac{r}{a}\right) \geq \sqrt{1 - \left(\frac{NA}{n_{co}\sin\theta}\right)^2} \frac{1}{\sin\varphi} = \left(\frac{r}{a}\right)_L. \tag{9}$$

Since $(r/a) \leq 1$,

$$\sin\varphi \geq \sqrt{1 - \left(\frac{NA}{n_{co}\sin\theta}\right)^2} = \sin\varphi_L. \tag{10}$$

With these relationships, the contribution to the trapped energy from wide-angle rays is, including the prefactors,

$$P_W = 8\pi^2 a^2 \rho pI \left[\left(\frac{\pi}{2}\right)\left(\frac{n_{cl}}{n_{co}}\right) - \int_{\theta_L}^{\theta_U} \sin\theta \sin^{-1}\sqrt{1 - \left(\frac{NA}{n_{co}\sin\theta}\right)^2} d\theta - \left(\frac{NA}{n_{co}}\right)\int_{\theta_L}^{\theta_U} \sqrt{1 - \left(\frac{NA}{n_{co}\sin\theta}\right)^2} d\theta\right]. \tag{11}$$

Let us define the two integrals in Eq. (11) as I_1 and I_2. Then we can rewrite the equation as

$$P_W = 8\pi^2 a^2 \rho pI\left[\left(\frac{\pi}{2}\right)\left(\frac{n_{cl}}{n_{co}}\right) - I_1 - \left(\frac{NA}{n_{co}}\right) I_2\right]. \tag{12}$$

By combining a certain amount of ingenuity with standard integration techniques, one can prove,[10] for these particular limits of integration, that both integrals in Eq. (12) are equal to

$$I_1 = I_2 = \left(\frac{\pi}{2}\right)[1 - \sqrt{1 - (n_{cl}/n_{co})^2}]. \tag{13}$$

By plugging this expression into Eq. (12), it readily follows that

$$P_W = 4\pi^2 a^2 \rho pI\left(\frac{n_{cl}}{n_{co}}\right)\left[1 - \left(\frac{n_{cl}}{n_{co}}\right)\right]. \tag{14}$$

In addition, by combining this equation with Eq. (6), we obtain

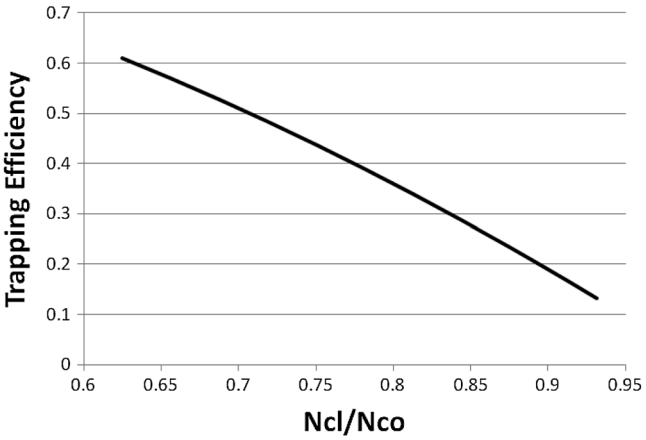

Fig. 6 Trapping efficiency (TE) versus n_{cl}/n_{co} [TE = $1 - (n_{cl}/n_{co})^2$].

$$P_W = P_N\left(\frac{n_{cl}}{n_{co}}\right). \tag{15}$$

This equation tells us that as (n_{cl}/n_{co}) diminishes, the relative contribution from the wide-angle rays also diminishes. This trend occurs because, as the ratio of the two indices drops, the narrow angle widens and the wide angle narrows. For the Saint Gobain fiber, where the core and cladding indices are 1.6 and 1.49, respectively, the contribution to the fluorescence power from the wide-angle rays is ~93% of that from the narrow-angle rays. Even at a cladding index = 1.0, the relative contribution is 62.5%.

The trapping efficiency (TE), as described at the beginning of this section, can be expressed as

$$TE = (P_W + P_N)/4\pi^2 a^2 \rho pl. \tag{16}$$

It then follows, using Eqs. (6), (15), and (16), that the TE is

$$TE = 1 - (n_{cl}/n_{co})^2. \tag{17}$$

We note that, within this treatment, the TE is independent of the volume density of fluorescers. This simple expression is plotted in Fig. 6. In this figure, the core index is the same as that of the Saint Gobain fiber, 1.6. The maximum cladding index is also the same as the Saint Gobain fiber, 1.49, and the minimum index is that of an air cladding, 1. The TE of the Saint Gobain fiber is ~13%, while for an air cladding, it is ~61%. The indices between these two are not included just to exhibit a trend; down to ~1.3, they can be achieved with various degrees of fluorination of conventional polymers, for which $n_{cl}/n_{co} = 0.8125$. Indices <1.3 to values <1.1 can be achieved by creating nanopores (i.e., small empty spaces) in a material such as silica.[11]

5 Conclusion

The TE of a fluorescent optical fiber has been calculated, assuming a uniform distribution of fluorescers over the cross-sectional area of the fiber, a uniform excitation of the fluorescers, and a uniform emission of fluorescence radiation over a solid angle. These assumptions are reasonable but could be relaxed. The calculation includes the contribution from rays over the full range of azimuth and those that are

guided over only part of that range. The rays in the latter category make a substantial contribution to the total, but less than half, which diminishes along with the ratio of the cladding-to-core index. Furthermore, a simple analytic expression for the TE is presented.

References

1. A. D. Bross, "Scintillating plastic optical fiber radiation detectors in high-energy particle physics," *Proc. SPIE* **1592**, 122–132 (1991).
2. J. C. Thevenin et al., "Scintillating and fluorescent plastic optical fibers for sensors applications," *Proc. SPIE* **0514**, 133–142 (1984).
3. N. A. Amos, A. D. Bross, and M. C. Lundin, "Optical attenuation length measurements of scintillating fibers," *Instrum. Methods Phys. Res. A* **297**(3), 396–403 (1990).
4. B. Abbot et al., "Scintillating fibers and waveguides for tracking applications," *IEEE Trans. Nucl. Sci.* **38**(2), 441–445 (1991).
5. G. F. Knoll, "Scintillation detection principles," Chapter 8 in *Radiation Detection and Measurement*, 4th ed., pp. 261–270, Wiley, Hoboken, NJ (2010).
6. J. D. Weiss, "A fluorescent long-line fiber-optic position sensor," *Sens. Mag.* **22**(3), 28–32 (2005).
7. http://zeus.phys.uconn.edu/halld/tagger/fp-microscope/SGC_Scintillating_Optical_Fibers_Brochure_605.pdf (12 February 2015).
8. www.nanoptics.com (12 February 2015).
9. A. W. Snyder and J. D. Love, "Leaky rays," Chapter 7 in *Optical Waveguide Theory*, 1st ed., pp. 134–153, Chapman and Hall, London, England (1983).
10. J. O. Mercer, National Council of Teachers of Mathematics, private communication (2014).
11. "Low & ultra-low refractive index polymers," (17 January 2011), http://omnexus.specialchem.com/tech-library/article/low-ultra-low-refractive-index-polymers (12 February 2015).

Jonathan D. Weiss is the chief technology officer of JSA Photonics LLC, a small high-technology company in Corrales, New Mexico. The company specializes in optical sensors. Before coming to JSA, he worked as a physicist at Sandia National Laboratories, where much of his work was in the area of optical sensors. He holds seventeen patents for such sensors, several of which have been licensed to private industry.